ACSNANO

www.acsnano.org

ARTICLE

Ion Accumulation and Migration Effects on Redox Cycling in Nanopore Electrode Arrays at Low Ionic Strength

Chaoxiong Ma,[†] Wei Xu,[†] William R. A. Wichert,[†] and Paul W. Bohn*[,†,‡]

[†]Department of Chemistry and Biochemistry and [‡]Department of Chemical and Biomolecular Engineering, University of Notre Dame, Notre Dame, Indiana 46556, United States

Supporting Information

ABSTRACT: Ion permselectivity can lead to accumulation in zero-dimensional nanopores, producing a significant increase in ion concentration, an effect which may be combined with unscreened ion migration to improve sensitivity in electrochemical measurements, as demonstrated by the enormous current amplification (~2000-fold) previously observed in nanopore electrode arrays (NEA) in the absence of supporting electrolyte. Ionic strength is a key experimental factor that governs the magnitude of the additional current amplification (AF_{ad}) beyond simple redox cycling through both ion accumulation and ion migration effects. Separate contributions from ion accumulation and ion migration to the overall AF_{ad} were identified by studying NEAs with varying geometries, with larger AF_{ad} values being achieved in NEAs with smaller pores. In addition, larger AF_{ad} values were observed for $Ru(NH_3)_6^{3/2+}$ than for ferrocenium/ferrocene (Fc^+/Fc) in aqueous solution, indicating that coupling efficiency in redox cycling can significantly affect AF_{ad}. While charged species are required to observe migration effects or ion accumulation, poising the top electrode at an oxidizing potential converts neutral species to cations, which can then exhibit current amplification similar to starting with the cation. The electrical double layer effect was also demonstrated for Fc/Fc^+ in acetonitrile and 1,2-dichloroethane, producing AF_{ad} up to 100× at low ionic strength. The pronounced AF_{ad} effects demonstrate the advantage of coupling redox cycling with ion accumulation and migration effects for ultrasensitive electrochemical measurements.

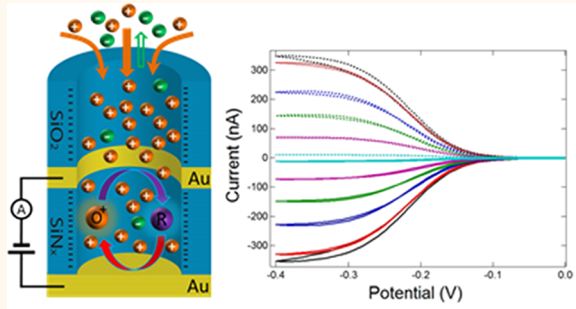

Ion Accumulation Coupled Redox Cycling in Nanopore Electrode

KEYWORDS: *redox cycling, nanopore electrode array, ion accumulation, ion migration, current amplification, electrical double layer effect*

Nanotechnology offers great possibilities for electrochemical sensing by enabling the fabrication of electrochemical devices with precise, controlled, nanometer-scale geometries, thus greatly expanding the repertoire of electrochemical experiments that exhibit nanoscale effects.[1−5] One important nanoscale effect arises when the interfacial electric fields—characterized by the electrical double layer (EDL) thickness or Debye length, λ_D,[6,7] which determines transport and redox reaction kinetics of charged species at an electrode−solution interface[8−12]—become large enough to interact with the surroundings. In a typical voltammetric measurement with excess supporting electrolyte (SE), λ_D is typically ~1 nm. Accordingly, ion migration effects resulting from the electric-field-driven ion transport are negligible at macroscopic electrodes, and diffusion is the dominant contribution to mass transport.[13−15] At low ionic strength, however, a significant depletion zone forms, accompanied by a sizable electric field, and if two electrodes are sufficiently close that their EDLs overlap, ion migration can contribute significantly to mass transport and thus to faradaic currents.[9,10,16−20] As a result, currents can be enhanced or diminished depending on the charge of the redox-active species and whether the electrode reaction increases or decreases it.[10,17,21,22]

In the absence of supporting electrolyte, a redox species at 1 μM exhibits λ_D ~ 200 nm, as determined from the Debye−Hückel approximation,[6,7] which is only a small fraction of the diffusive boundary layer for a macroscopic planar electrode.[23] However, in nanoscale dual-electrode structures, λ_D can be comparable to the interelectrode distance, and the overlapping EDLs can cause the redox dynamics at the two electrodes to be strongly coupled.[11,24−26] This concept has been exploited by White and co-workers, who studied ion transport in nanogap

Received: January 4, 2016
Accepted: February 24, 2016
Published: February 24, 2016

DOI: 10.1021/acsnano.6b00049
ACS Nano 2016, 10, 3658−3664

electrochemical cells in redox cycling (RC) mode,[27−31] which relies on the cycling of redox species locally between two electrodes.[11,24] As a result of ion generation and depletion on two biased electrodes, an electric field is established that affects the transport of charged species, tending to move them toward the oppositely charged electrode. In addition, the movement of the charged species can be affected by any *iR* drop across the top and bottom electrodes.

On the other hand, nanopores or nanochannels may also exhibit overlapping EDLs, leading to screening or enrichment of ions to balance the surface charge and maintain charge neutrality.[32−37] Due to the high surface-to-volume ratio of these nanostructures, permselectivity effects result in ion accumulation that can increase local ion concentrations by orders of magnitude, as demonstrated by electrical conductance[14,35] and fluorescence measurements.[34,38] Although nanopore electrodes and their arrays have been widely employed for electrochemical sensing,[2,3,39] this enormous ion enrichment effect has not been purposefully exploited to enhance faradaic currents. Indeed, the nanopore electrodes with controllable surface charge have been reported to increase the current of oppositely charged ions but decrease those of the same charge.[40−42] Observed current enhancements at single nanopore electrodes are modest, equivalent to only a small fraction of the ions accumulated within the nanopores.[40−43] This is because the ions accumulated inside the nanopores are insufficient to provide a steady-state response since the diffusive boundary layer at a single electrode is typically of micrometer dimensions in voltammetry.

In contrast, redox cycling between closely spaced dual generator and collector electrodes relies mainly on the localized concentration of the redox species.[26−28,30,44] By incorporating this principle, we recently demonstrated that it is possible to significantly improve measurable current by producing an additional current amplification factor (AF_{ad}), up to 100-fold, for $Ru(NH_3)_6^{2/3+}$ in the absence of SE in a nanopore electrode array (NEA) with 100 nm interelectrode spacing.[25] In the absence of supporting electrolyte, the ionic strength is low and is determined entirely by the redox-active species. Overlapping EDLs from the generator and collector electrodes augment the permselectivity of the nanopores to produce significant AF_{ad}, an effect that is attributed to the combined effects of ion migration and ion accumulation,[25] although the electric fields from the electrodes and nanopore surface do not act strictly independently.

In the present work, the underlying mechanism of this additional current amplification and its applicability to other systems is addressed by posing and answering several fundamental questions, including the following: (1) What are the relative contributions of the ion migration and ion accumulation effects? (2) Do similar effects occur for other cations? (3) Do the initial redox species have to be charged in order to observe AF_{ad}? (4) Can substantial AF_{ad} values be obtained in organic solvents? In order to differentiate ion migration and ion accumulation effects without fully decoupling the interactions of the electric fields, a simplified model was employed to characterize the behavior of NEAs with constant interelectrode spacing but different pore diameter, *d*, by assuming that (1) migration effects are relatively insensitive to *d* and (2) the nanopore charge density is inversely proportional to *d*.[36,45] The applicability of the NEA/EDL effect to other cations with different charge was studied using ferrocene/ferrocenium, Fc/Fc^+, as a model redox system. While previous studies showed that charge is required to observe either accumulation or migration effects in nanopores, it was not found to be necessary in the NEA geometry. Indeed, by holding the top electrode at an oxidizing potential, neutral species, such as ferrocenedimethanol, can be preoxidized and produce similar AF_{ad} values as Fc^+. Voltammetry in nonaqueous solvent was also investigated using ferrocene (Fc) dissolved in acetonitrile and dichloroethane.

RESULTS AND DISCUSSION

Nanopore electrode arrays, consisting of annular top and bottom electrodes separated by a nanometer-scale dielectric, were fabricated using a combination of metal evaporation, photolithographic patterning, nanosphere lithography (NSL), and reactive ion etching (RIE), as described previously.[25,44] The diameter, *d*, of the pores in the NEA was controlled by the size of the spheres used to define the NSL pattern and the time of the subsequent RIE exposure. Figure 1 illustrates the fabrication of the NEAs and scanning electron microscopy (SEM) images of the arrays at two different magnifications.

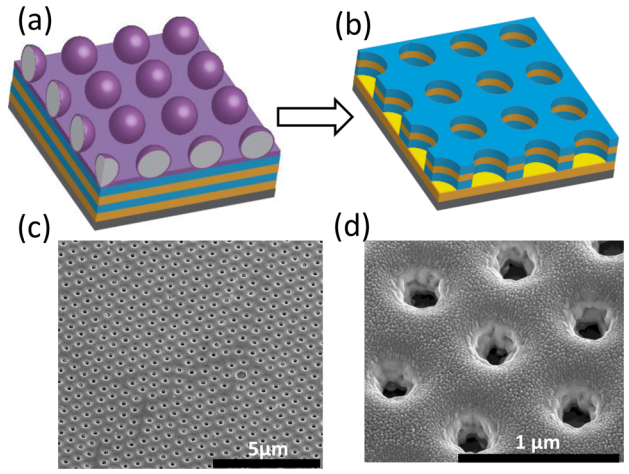

Figure 1. Schematic diagram showing the fabrication of the NEA device after layer-by-layer deposition and NSL (a) and after the multistep RIE process (b). Colors are used to represent different layers: black (glass slide), yellow (Au), blue (SiN_x or SiO_2), and purple (polystyrene sphere or Cr). SEM image of the NEA at 30° tilt with $d \sim 300$ nm (c) and a magnified view (d).

Effect of Ionic Strength. Ionic strength has been demonstrated to govern the effects of ion migration and ion accumulation in nanopores, altering the limiting current (i_{lim}) in voltammetry upon the removal of SE.[11,19,46,47] Cyclic voltammetry (CV) with varying SE concentration was performed for $Ru(NH_3)_6^{3+}$ on an NEA with a pore diameter of 300 nm in redox cycling mode by holding the top and bottom electrodes at oxidizing and reducing potentials for $Ru(NH_3)_6^{3/2+}$, respectively. As shown in Figure 2, a decrease in limiting current was observed at all $Ru(NH_3)_6^{3/2+}$ concentrations with increasing KCl (background electrolyte) concentration. This observation can be attributed to the fact that both ion migration and ion accumulation effects become smaller with increasing ionic strength and shorter Debye length, λ_D. At higher ionic strengths, K^+ ions compete with $Ru(NH_3)_6^{3/2+}$ to compensate the negatively charged nanopore surface, thereby decreasing the concentration of $Ru(NH_3)_6^{3/2+}$ in the pores (ion accumulation effect). On the other hand, ion migration

DOI: 10.1021/acsnano.6b00049
ACS Nano 2016, 10, 3658−3664

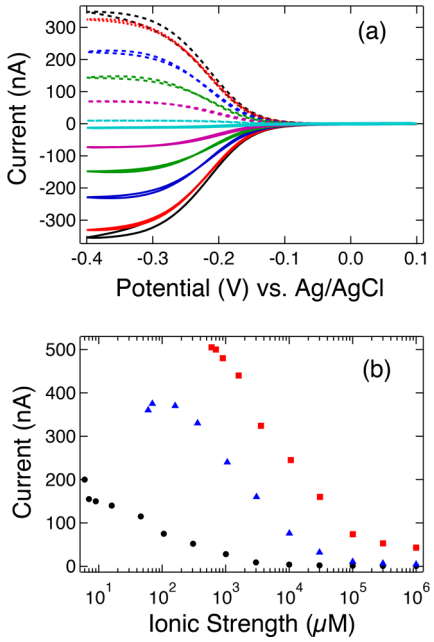

Figure 2. (a) Cyclic voltammograms of 10 μM $Ru(NH_3)_6^{3+}$ in the presence of 0 mM (black), 0.3 mM (red), 1 mM (blue), 3 mM (green), 10 mM (purple), and 100 mM (cyan) KCl. Current at the bottom electrode (solid) and top electrode (dashed). Triangular waveform is applied to the bottom electrode at a scan rate of 100 mV/s, while the top electrode is maintained at +0.1 V *vs* Ag/AgCl. (b) Limiting current of CVs obtained from $Ru(NH_3)_6^{3+}$ at 1 μM (black), 10 μM (blue), and 100 μM (red) concentration as a function of ionic strength.

facilitates the movement of $Ru(NH_3)_6^{3+}$ to the bottom electrode (cathode) for its reduction, which is the rate-limiting step for ion transport and redox cycling. Thus, as the ionic strength increases, shielding effects increase, reducing the ion migration contribution to mass transport of the redox-active moieties. Both effects interact additively to reduce the voltammetric response and resulting current with increasing ionic strength.

At 1.0 μM $Ru(NH_3)_6^{3+}$, a combination of these two effects leads to a ~280-fold increase of AF_{ad}, obtained by comparing the limiting current obtained in the absence of SE (i_{ASE}, 200 nA) and that obtained in 1.0 M KCl (i_{SE}, 0.7 nA).

$$AF_{ad} = \frac{i_{ASE}}{i_{SE}} \quad (1)$$

The AF_{ad} obtained here is 2.8× larger than that previously observed (~100×) on a similar nanopore electrode array.[25] This is likely the result of smaller nanopores in the NEA, which produce a larger accumulation effect and resulting current amplification. It is interesting to note that this accumulation process, indicated by the increase of limiting current with scan number, can be observed for measurements at low ionic strength[25] (see Figure S1, Supporting Information, SI). At higher $Ru(NH_3)_6^{3+}$ concentration, smaller AF_{ad} values are observed because the larger analyte concentration produces a higher ionic strength in the absence of SE and correspondingly smaller ion migration and accumulation effects.

Contributions from Ion Migration and Accumulation. The strong dependence of AF_{ad} on pore size suggests a way to separate the contributions from ion migration and ion accumulation to the overall additional current amplification based on the assumptions mentioned above. The Debye length, λ_D, corresponding to $Ru(NH_3)_6^{3+}$ solutions in the range of 1−100 μM is 150−15 nm in the absence of SE,[6] values which are comparable to the interelectrode distance, h = 100 nm, and pore diameter, d = 300 nm. As a result, both ion migration and accumulation can potentially contribute to the current enhancement due to the overlapping EDLs. Migration effects should depend primarily on the distance between top and bottom electrodes, which was held constant at 100 nm in this study. Ion accumulation, on the other hand, depends strongly on the pore diameter, d, and can be characterized by equilibrium ion concentration in nanopore, C_e[45]

$$C_e = C_0 + C_s = C_0 + 10^{-3}\frac{2\sigma_s^*}{dN_A Ze} \quad (2)$$

where C_0 and C_s are the contribution of ions from bulk solution and charged surface to C_e, respectively, σ_s^* is the surface charge density, and Z is the charge of the ionic species.

In order to differentiate the contributions from ion migration and ion accumulation, AF_{ad} values were obtained from electrode arrays with different pore diameters, d, and compared. Figure 3 illustrates the dependence of AF_{ad} on pore diameter.

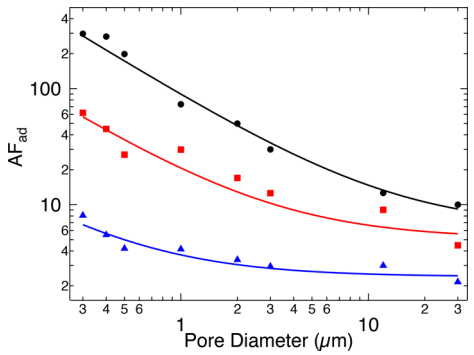

Figure 3. Additional current amplification (AF_{ad}) obtained for $Ru(NH_3)_6^{3+}$ solutions at 1 μM (black circle), 10 μM (red square), and 100 μM (blue triangle) concentration as a function of pore diameter. A scan rate of 100 mV/s was used for all CV measurements. Solid lines represent fits of the data to eq 5.

As expected, AF_{ad} decreases with increasing d at all three $Ru(NH_3)_6^{3+}$ concentrations, which is attributed primarily to decreasing accumulation and a smaller resulting C_e. Since the current amplification is the combination of ion migration (AF_m), which is considered to be independent of d, and ion accumulation (AF_a), the additional amplification factor (AF_{ad}) is given by

$$AF_{ad} = AF_m \times AF_a \quad (3)$$

If we assume that the limiting current obtained in the redox cycling mode is proportional to localized ion concentration, C_e, the contribution of ion accumulation can be expressed using the ratio of the ion concentration inside the pores and bulk solution

$$AF_a = \frac{C_e}{C_0} = 1 + \frac{k_s}{d} \quad (4)$$

where $k_s = 10^{-3}\frac{2\sigma_s^*}{N_A ZeC_0}$ is invariant under constant measurement conditions. AF_{ad} can then be rewritten as

DOI: 10.1021/acsnano.6b00049
ACS Nano 2016, 10, 3658−3664

$$AF_{ad} = AF_m\left(1 + \frac{k_s}{d}\right) \quad (5)$$

In an array with a sufficiently large pore diameter, migration becomes the dominant contribution since ion accumulation is negligible (*i.e.*, $k_s \ll d$). The data in Figure 3 are fit to eq 5, and the recovered values of AF_m and AF_a for a d = 300 nm NEA are given in Table 1. Reasonable agreement of the experimental data with the proposed model justifies the use of these assumptions to identify the contributions of ion migration and accumulation to the overall current amplification. Although the electric fields on electrodes and within nanopores can interact with each other at low ionic strength, their coupling is not large enough to affect the individual contributions of ion migration and accumulation.

Table 1. Ion Accumulation (AF_a) and Ion Migration (AF_m) Contributions to AF_{ad} for a d = 300 nm NEA

$[Ru(NH_3)_6^{3+}]$	1 μM	10 μM	100 μM
AF_a	43.4	10.2	1.8
AF_m	6.4	5.1	2.4
AF_{ad}	284	57	7

AF_m is ~6 for 1 μM $Ru(NH_3)_6^{3+}$, which is larger than typical values reported on planar macroscopic electrodes for ions of the same charge.[16,22] We attribute the difference to the open nanopore geometry of the array. Diffusion of redox-active species to the bottom electrode is the rate-limiting step for redox cycling because the top electrode is more accessible to bulk solution. Therefore, the migration effect that facilitates transport of $Ru(NH_3)_6^{3+}$ ions to the negatively charged bottom electrode significantly enhances the efficiency of redox cycling, resulting in a larger migration contribution than that obtained from a macroscopic electrode with a distant reference electrode. While both AF_a and AF_m decrease with the increase of $Ru(NH_3)_6^{3+}$ concentration, AF_a decreases more dramatically because the smaller λ_D and resulting EDL affect permselectivity and ion transport to the nanopore more strongly than transport between the electrodes.

Effect of Ion Charge. Previous studies have demonstrated that ion migration effects in voltammetry and ion accumulation in nanopores depend strongly on the charge of the redox-active species.[13,14,16,38] To understand how ion charge affects AF_{ad}, ferrocenium (Fc^+), a singly charged cation, was used as the analyte. Figure 4 shows the results of i_{lim} obtained from different Fc^+ concentrations in aqueous solution in the presence and absence of 0.1 M KCl. Similar to the results obtained for $Ru(NH_3)_6^{3+}$,[25] three distinct regions of behavior that depend on the ionic strength are observed for the measurement of Fc^+ in the absence SE. At high analyte concentration (region III), there is little difference between the behavior with and without SE since the ionic strength is high whether or not there is SE. At 3 μM < C_0 < 100 μM (region II), i_{ASE} is obviously larger than i_{SE} and changes only slightly with C_0. This is attributed to a combination of ion accumulation and migration effects resulting from partially overlapping EDL, which counteracts the decrease of electroactive Fc^+ concentration, leading to a slow change of i_{lim}. As C_0 is further decreased below 3 μM, a quasi-linear response is observed (region I). This is consistent with the results of $Ru(NH_3)_6^{3+}$ and can be attributed to ion competition and a relatively constant migration effect due to the completely overlapping EDL.[25] The AF_{ad} value obtained in region I is ~10, which is smaller than the approximate 100-fold effect obtained for $Ru(NH_3)_6^{3+}$ but higher than the values reported previously for singly charged ions measured on macroscopic planar electrodes or in ultrathin layer cells.[21,22] Since Fc^+ is reduced to a neutral species, ferrocene (Fc), which is not accumulated in the nanopores, redox cycling of Fc^+/Fc is coupled less efficiently than the $Ru(NH_3)_6^{3/2+}$ system, in which both redox partners are accumulated. This difference is more obvious at low C_0, where ion competition is no longer negligible because Fc^+ is a weaker competitor than $Ru(NH_3)_6^{3/2+}$ for accumulation on the negatively charged nanopore surface. Nevertheless, this current amplification is significantly larger than that produced on a macroscopic planar electrode, demonstrating the advantage of using the NEA architecture for exploring the EDL effect.

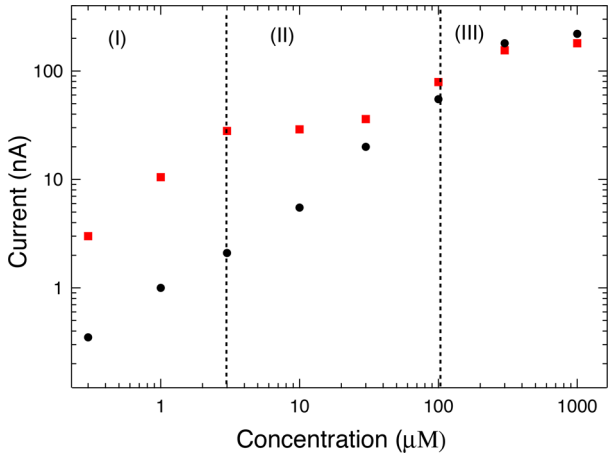

Figure 4. Limiting current of cyclic voltammograms of aqueous solutions of ferrocenium as a function of concentration in 0.1 M KCl (black) and in the absence of SE (red) measured at 100 mV/s.

At high concentration region (C_0 > 100 μM), i_{lim} deviates significantly from a linear response, exhibiting obviously smaller currents than that expected in the presence or absence of SE. This may be ascribed to the low solubility of ferrocene in aqueous solution, resulting in the formation of solid ferrocene from the reduction of Fc^+, as evidenced by the peak-shaped CV response obtained at $C_0 \geq 300$ μM (see Figure S2, SI).

Since the electric field affects only the transport of charged species, ion migration and accumulation are exclusively observed for ionic species.[14,16,36,38] In a nanopore array with dual electrodes, it is possible to preoxidize a neutral species to a cationic species on the top electrode to enable the ion accumulation and migration effect. In order to demonstrate this concept on NEAs, ferrocenedimethanol (FcDM) was used as the redox-active species. Figure 5 shows the results obtained with relatively negative (E_T = 0 V) and positive (E_T = +0.5 V) potentials applied to the top electrode. In the presence of SE, no obvious differences are observed for i_{lim} obtained at E_T = +0.5 V and E_T = 0 V, which is consistent with previous results reported on similar RC electrode geometries and thin-layer cells.[30,44,48] Consistent with previous observations for redox cycling measurements,[19,27,44] a larger charging current is seen for the bottom electrode than for the top electrode held at constant potential. The hysteresis effect is more severe in the presence of SE (0.1 M KCl) which supports the charging process. In addition, an offset reduction current (~6 nA) is observed at the top electrode held at 0 V (red dash), which is not collected by the bottom electrode. This is likely due to a

DOI: 10.1021/acsnano.6b00049
ACS Nano 2016, 10, 3658−3664

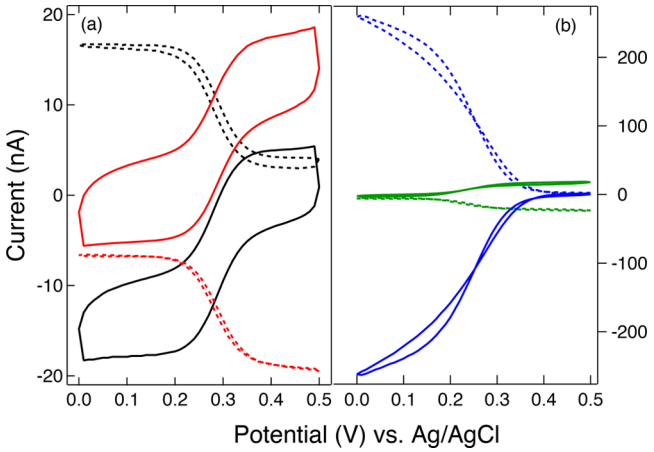

Figure 5. (a) Cyclic voltammograms at a scan rate of 100 mV/s for an aqueous solution of 0.1 mM ferrocenedimethanol in the presence of 0.1 M KCl with E_T = 0 V (red) and E_T = 0.5 V (black) *vs* Ag/AgCl. (b) Cyclic voltammograms in the absence of SE with E_T = 0 V (green) and E_T = 0.5 V (blue) *vs* Ag/AgCl. Current measured at bottom electrode (solid) and top electrode (dashed).

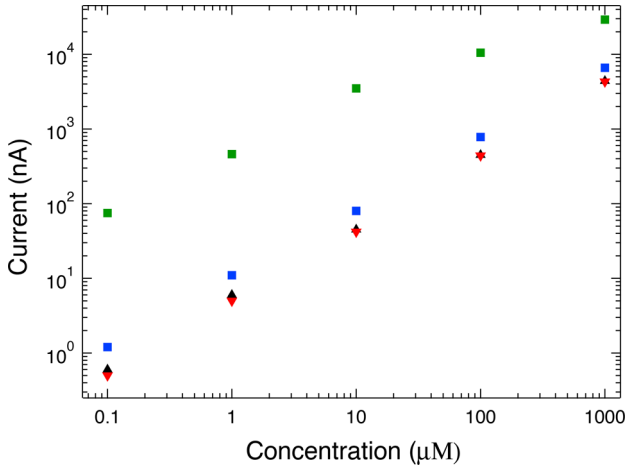

Figure 6. Limiting currents obtained from voltammograms of ferrocene in acetonitrile as a function of concentration in 0.1 M $TBAPF_6$ (triangles) with E_T = 0 V (black) and E_T = +0.6 V (red) and in the absence of SE (squares) with E_T = 0 V (blue) and E_T = +0.6 V (green). A scan rate 100 mV/s was used for all CV measurements, and all potentials are referenced to Ag/AgCl.

combination of irreversible impurities in the FcDM and dissolved oxygen from the atmosphere. In the absence of SE, i_{lim} at E_T = 0 V is ~1.5-fold larger than those measured in the presence of SE, indicating a small contribution from ion accumulation and migration. On the other hand, at E_T = +0.5 V i_{lim} is 10-fold higher than that obtained at E_T = 0 V in the absence of SE. This current amplification and resulting AF_{ad} are comparable to that produced using Fc^+ as the analyte (Figure 4) and are assigned to a combination of both ion accumulation and ion migration effects. By holding the top electrode at an anodic potential, conversion of FcDM to its oxidized form ($FcDM^+$) enables its enrichment by ion accumulation in the nanopores and facilitates its transport to the bottom electrode due to ion migration.

Effect of Solvent. To explore whether voltammetry in organic solvents shows migration and accumulation effects similar to those observed in aqueous solutions, we examined the changes in ion transport upon the removal of SE in acetonitrile.[9,47] Eliminating the SE could be advantageous for voltammetry in nonaqueous solutions because supporting electrolytes suitable for organic solvents are typically expensive and plagued by problems of low solubility.[10] Ion permselectivity has been observed in nanopores in organic systems, producing limiting currents that depend strongly on SE concentration.[40,41] In order to investigate the voltammetry of NEAs at low ionic strength in an organic solvent, ferrocene (Fc) in acetonitrile was used as a model system. As illustrated in Figure 6, i_{lim} obtained in the presence of tetrabutylammonium hexafluorophosphate ($TBAPF_6$) responds linearly to the Fc concentration and shows negligible dependence on the potential of top electrode (E_T). In the absence of the $TBAPF_6$ SE, relatively negative potentials at the top electrode (E_T = 0 V) produce i_{lim} (1.5−2×) slightly larger than that obtained in the presence of SE, which is likely due to a small contribution of ion accumulation and ion migration.

In contrast, much more pronounced effects are observed when an oxidizing potential (E_T = +0.6 V) is applied to the top electrode, producing a much larger i_{lim} compared to that obtained in the presence of SE, especially at low Fc concentrations. Increases in AF_{ad} as large as 100-fold were observed at C_0 < 10 μM as a result of both accumulation of Fc^+ generated at the top electrode (E_T = +0.6 V) as well as migration enhancing transport of Fc^+ to the bottom electrode. The accumulation process is also supported by a transient effect observed in CV measurements of Fc at low ionic strength with E_T = +0.6 V, similar to that observed for charged species, $Ru(NH_3)_6^{3+}$ (see Figures S1 and S3, SI). The dependence of i_{lim} on E_T is identical to that observed in the aqueous solution (Figure 4). The AF_{ad} obtained in acetonitrile is larger than that observed in aqueous solution, an observation that can be explained by fewer competing ions in acetonitrile. In particular, ionic interferences arising from CO_2 dissolution (producing H^+ and HCO_3^-) and K^+ leaking from the reference electrode are less likely to occur in organic solvent. Low ionic strength measurements were also performed with Fc/Fc^+ in 1,2-dichloroethane, which produces similar AF_{ad} (~100) at C_0 = 0.1 μM (see Figure S4, SI). These results suggest that the overlapping EDL effect in the NEA geometry combined with redox cycling can deliver enhanced voltammetric measurements in organic systems, eliminating the need for SE, while providing even higher sensitivity.

CONCLUSIONS

Redox cycling in nanopore electrode arrays in the absence of SE yields additional current amplification, AF_{ad}, up to 280-fold, which is attributed to a combination of ion migration and ion accumulation resulting from overlapping EDLs. Separate contributions from ion accumulation and ion migration to the overall AF_{ad} were identified by studying NEAs with varying geometries. Larger AF_{ad} values are achieved in NEAs with smaller pores because they support higher ion accumulation. In addition, larger AF_{ad} values are observed for $Ru(NH_3)_6^{3/2+}$ than for Fc^+/Fc in aqueous solution, suggesting that coupling efficiency in redox cycling, which relies on charge and solubility of the redox couple, can significantly affect AF_{ad}. While charged species are required to observe migration effects or ion accumulation, poising the top electrode at an oxidizing potential converts neutral species to cations, which can then exhibit current amplification similar to starting with the cation.

DOI: 10.1021/acsnano.6b00049
ACS Nano 2016, 10, 3658−3664

The EDL effect was also demonstrated for Fc/Fc^+ in acetonitrile and 1,2-dichloroethane, producing AF_{ad} up to 100× at low ionic strength. The fact that large AF_{ad} values are observed in the NEA geometry with different redox pairs, NEA dimensions, ionic strengths, and solvents demonstrates the universality of the phenomenon at the nanoscale and the advantages of nanopore electrodes for coupling the EDL effect with redox cycling to produce ultrasensitive electrochemical measurements at low ionic strength. The strategy employed here eliminates the need for the addition of SE in voltammetry and also achieves 1−2 orders magnitude higher sensitivity. Although the model systems described here all used cationic species in negatively charged nanopores, similar EDL effects and AF_{ad} are expected for anodic species in positively charged pores.

EXPERIMENTAL SECTION

Device Fabrication. The NEAs were fabricated using a procedure modified slightly from the one described previously.[44,49] Briefly, layer-by-layer deposition was used to create the NEAs, which consist of two 200 nm thick Au film electrodes (top and bottom) separated by 100 nm of SiN_x and covered with a 200 nm layer of SiO_2. Polystyrene (PS) spheres and Cr film were used to define the pattern for reactive ion etching (RIE). The pore diameter, d, was controlled by the size of PS spheres, and they were reduced in diameter in a subsequent RIE step. NEAs with d = 300 nm were used for all the experiments, except in the studies of pore size dependence, which were controlled accordingly (see SI). Upon removing the PS spheres with chloroform, the SiO_2, top Au, and SiN_x layers of the device were etched using a multistep RIE process. A schematic diagram of the array before and after RIE and SEM images of the NEA are given in Figure 1. The array size is typically 100 μm × 100 μm.

Electrochemical Characterization. Cyclic voltammetry experiments were conducted on a CHI bipotentiostat (842c, CH Instruments Inc.) using a platinum wire and a Ag/AgCl electrode as auxiliary and reference electrodes, respectively. In all CV measurements, the top electrode is held at a constant potential (RC mode) or floating (non-RC mode), while the potential of the bottom electrode is scanned at 100 mV/s. Limiting current obtained from the bottom electrode is used for the figures and discussion.

ASSOCIATED CONTENT

Supporting Information

The Supporting Information is available free of charge on the ACS Publications website at DOI: 10.1021/acsnano.6b00049.

Fabrication of NEAs with different pore diameters and electrochemical measurements in different solvent conditions (PDF)

AUTHOR INFORMATION

Corresponding Author

*E-mail: pbohn@nd.edu.

Notes

The authors declare no competing financial interest.

ACKNOWLEDGMENTS

This work was supported by the National Science Foundation through Grant 1404744 (C.M.) and the Department of Energy Office of Science through Grant DE FG02 07ER15851 (W.X. and W.R.A.W.). We gratefully acknowledge L. Zaino for valuable discussions. Fabrication and structural characterization of the devices studied here were accomplished at the Notre Dame Nanofabrication Facility and the Notre Dame Integrated Imaging Facility, whose generous support is gratefully acknowledged.

REFERENCES

(1) Murray, R. W. Nanoelectrochemistry: Metal Nanoparticles, Nanoelectrodes, and Nanopores. *Chem. Rev.* **2008**, *108*, 2688−2720.
(2) Oja, S. M.; Wood, M.; Zhang, B. Nanoscale Electrochemistry. *Anal. Chem.* **2013**, *85*, 473−486.
(3) Dawson, K.; O'Riordan, A. Electroanalysis at the Nanoscale. *Annu. Rev. Anal. Chem.* **2014**, *7*, 163−181.
(4) Lemay, S. G.; Kang, S.; Mathwig, K.; Singh, P. S. Single-Molecule Electrochemistry: Present Status and Outlook. *Acc. Chem. Res.* **2013**, *46*, 369−377.
(5) Penner, R. M. Chemical Sensing with Nanowires. *Annu. Rev. Anal. Chem.* **2012**, *5*, 461−485.
(6) Myers, D. *Surfaces, Interfaces, and Colloids*; Wiley-VCH: New York, 1999.
(7) Bard, A. J.; Faulkner, L. R. *Electrochemical Methods: Fundamentals and Applications*, 2nd ed.; John Wiley & Sons: New York, 2001; pp 156−176.
(8) Norton, J. D.; White, H. S.; Feldberg, S. W. Effect of the Electrical Double Layer on Voltammetry at Microelectrodes. *J. Phys. Chem.* **1990**, *94*, 6772−6780.
(9) Cooper, J. B.; Bond, A. M. Microelectrode Studies in the Absence of Deliberately Added Supporting Electrolyte: Solvent Dependence for a Neutral and Singly Charged Species. *J. Electroanal. Chem. Interfacial Electrochem.* **1991**, *315*, 143−60.
(10) Ciszkowska, M.; Stojek, Z. Voltammetric and Amperometric Detection without Added Electrolyte. *Anal. Chem.* **2000**, *72*, 754A−760A.
(11) Xiong, J.; Chen, Q.; Edwards, M. A.; White, H. S. Ion Transport within High Electric Fields in Nanogap Electrochemical Cells. *ACS Nano* **2015**, *9*, 8520−8529.
(12) Dickinson, E. J. F.; Compton, R. G. Influence of the Diffuse Double Layer on Steady-State Voltammetry. *J. Electroanal. Chem.* **2011**, *661*, 198−212.
(13) Amatore, C.; Fosset, B.; Bartelt, J.; Deakin, M. R.; Wightman, R. M. Electrochemical Kinetics at Microelectrodes. Part V. Migrational Effects on Steady or Quasi-Steady-State Voltammograms. *J. Electroanal. Chem. Interfacial Electrochem.* **1988**, *256*, 255−68.
(14) Stein, D.; Kruithof, M.; Dekker, C. Surface-Charge-Governed Ion Transport in Nanofluidic Channels. *Phys. Rev. Lett.* **2004**, *93*, 035901.
(15) Streeter, I.; Compton, R. G. Numerical Simulation of Potential Step Chronoamperometry at Low Concentrations of Supporting Electrolyte. *J. Phys. Chem. C* **2008**, *112*, 13716−13728.
(16) Cooper, J. B.; Bond, A. M.; Oldham, K. B. Microelectrode Studies without Supporting Electrolyte: Model and Experimental Comparison for Singly and Multiply Charged Ions. *J. Electroanal. Chem.* **1992**, *331*, 877−895.
(17) Oldham, K. B. Theory of Steady-State Voltammetry without Supporting Electrolyte. *J. Electroanal. Chem.* **1992**, *337*, 91−126.
(18) Zhang, Y.; Zhang, B.; White, H. S. Electrochemistry of Nanopore Electrodes in Low Ionic Strength Solutions. *J. Phys. Chem. B* **2006**, *110*, 1768−1774.
(19) Bartelt, J. E.; Deakin, M. R.; Amatore, C.; Wightman, R. M. Construction and Use of Paired and Triple Band Microelectrodes in Solutions of Low Ionic Strength. *Anal. Chem.* **1988**, *60*, 2167−2169.
(20) Bund, A.; Kubeil, C. Double Layer Effects at Nanosized Electrodes†. *Faraday Discuss.* **2013**, *164*, 339−348.
(21) Myland, J. C.; Oldham, K. B. Limiting Currents in Potentiostatic Voltammetry without Supporting Electrolyte. *Electrochem. Commun.* **1999**, *1*, 467−471.
(22) Ciszkowska, M.; Stojek, Z. Voltammetry in Solutions of Low Ionic Strength. Electrochemical and Analytical Aspects. *J. Electroanal. Chem.* **1999**, *466*, 129−143.
(23) Oldham, K. B. Theory of Microelectrode Voltammetry with Little Electrolyte. *J. Electroanal. Chem. Interfacial Electrochem.* **1988**, *250*, 1−21.

DOI: 10.1021/acsnano.6b00049
ACS Nano 2016, 10, 3658−3664

(24) Fan, L.; Liu, Y.; Xiong, J.; White, H. S.; Chen, S. Electron-Transfer Kinetics and Electric Double Layer Effects in Nanometer-Wide Thin-Layer Cells. *ACS Nano* **2014**, *8*, 10426−10436.
(25) Ma, C.; Contento, N. M.; Bohn, P. W. Redox Cycling on Recessed Ring-Disk Nanoelectrode Arrays in the Absence of Supporting Electrolyte. *J. Am. Chem. Soc.* **2014**, *136*, 7225−7228.
(26) Hyk, W.; Stojek, Z. Thin and Ultra-Thin Layer Dual Electrode Electrochemistry: Theory of Steady-State Voltammetry without Supporting Electrolyte. *Electrochem. Commun.* **2013**, *34*, 192−195.
(27) Niwa, O.; Morita, M.; Tabei, H. Electrochemical Behavior of Reversible Redox Species at Interdigitated Array Electrodes with Different Geometries: Consideration of Redox Cycling and Collection Efficiency. *Anal. Chem.* **1990**, *62*, 447−452.
(28) Sun, P.; Mirkin, M. V. Electrochemistry of Individual Molecules in Zeptoliter Volumes. *J. Am. Chem. Soc.* **2008**, *130*, 8241−8250.
(29) Wolfrum, B.; Zevenbergen, M.; Lemay, S. Nanofluidic Redox Cycling Amplification for the Selective Detection of Catechol. *Anal. Chem.* **2008**, *80*, 972−977.
(30) Zevenbergen, M. A. G.; Wolfrum, B. L.; Goluch, E. D.; Singh, P. S.; Lemay, S. G. Fast Electron-Transfer Kinetics Probed in Nanofluidic Channels. *J. Am. Chem. Soc.* **2009**, *131*, 11471−11477.
(31) Ma, C.; Zaino, L. P., III; Bohn, P. W. Self-Induced Redox Cycling Coupled Luminescence on Nanopore Recessed Disk-Multiscale Bipolar Electrodes. *Chem. Sci.* **2015**, *6*, 3173−3179.
(32) Hou, X.; Guo, W.; Jiang, L. Biomimetic Smart Nanopores and Nanochannels. *Chem. Soc. Rev.* **2011**, *40*, 2385−2401.
(33) Piruska, A.; Gong, M.; Sweedler, J. V.; Bohn, P. W. Nanofluidics in Chemical Analysis. *Chem. Soc. Rev.* **2010**, *39*, 1060−1072.
(34) Zhou, K.; Kovarik, M. L.; Jacobson, S. C. Surface-Charge Induced Ion Depletion and Sample Stacking near Single Nanopores in Microfluidic Devices. *J. Am. Chem. Soc.* **2008**, *130*, 8614−8616.
(35) Nam, S.-W.; Rooks, M. J.; Kim, K.-B.; Rossnagel, S. M. Ionic Field Effect Transistors with Sub-10 nm Multiple Nanopores. *Nano Lett.* **2009**, *9*, 2044−2048.
(36) Daiguji, H.; Yang, P.; Majumdar, A. Ion Transport in Nanofluidic Channels. *Nano Lett.* **2004**, *4*, 137−142.
(37) Wang, G.; Zhang, B.; Wayment, J. R.; Harris, J. M.; White, H. S. Electrostatic-Gated Transport in Chemically Modified Glass Nanopore Electrodes. *J. Am. Chem. Soc.* **2006**, *128*, 7679−7686.
(38) Pu, Q.; Yun, J.; Temkin, H.; Liu, S. Ion-Enrichment and Ion-Depletion Effect of Nanochannel Structures. *Nano Lett.* **2004**, *4*, 1099−1103.
(39) Cox, J. T.; Zhang, B. Nanoelectrodes: Recent Advances and New Directions. *Annu. Rev. Anal. Chem.* **2012**, *5*, 253−272.
(40) Newton, M. R.; Bohaty, A. K.; White, H. S.; Zharov, I. Chemically Modified Opals as Thin Permselective Nanoporous Membranes. *J. Am. Chem. Soc.* **2005**, *127*, 7268−7269.
(41) Newton, M. R.; Bohaty, A. K.; Zhang, Y.; White, H. S.; Zharov, I. pH- and Ionic Strength-Controlled Cation Permselectivity in Amine-Modified Nanoporous Opal Films. *Langmuir* **2006**, *22*, 4429−4432.
(42) Wang, G.; Bohaty, A. K.; Zharov, I.; White, H. S. Photon Gated Transport at the Glass Nanopore Electrode. *J. Am. Chem. Soc.* **2006**, *128*, 13553−13558.
(43) Li, C.-Y.; Tian, Y.-W.; Shao, W.-T.; Chun-Ge, Y.; Wang, K.; Xia, X.-H. Solution pH Regulating Mass Transport in Highly Ordered Nanopore Array Electrode. *Electrochem. Commun.* **2014**, *42*, 1−5.
(44) Ma, C.; Contento, N. M.; Gibson, L. R.; Bohn, P. W. Redox Cycling in Nanoscale-Recessed Ring-Disk Electrode Arrays for Enhanced Electrochemical Sensitivity. *ACS Nano* **2013**, *7*, 5483−5490.
(45) Schoch, R. B.; Renaud, P. Ion Transport through Nanoslits Dominated by the Effective Surface Charge. *Appl. Phys. Lett.* **2005**, *86*, 253111.
(46) Liu, Y.; Zhang, Q.; Chen, S. The Voltammetric Responses of Nanometer-Sized Electrodes in Weakly Supported Electrolyte: A Theoretical Study. *Electrochim. Acta* **2010**, *55*, 8280−8286.
(47) Amatore, C.; Deakin, M. R.; Wightman, R. M. Electrochemical Kinetics at Microelectrodes: Part Iv. Electrochemistry in Media of Low Ionic Strength. *J. Electroanal. Chem. Interfacial Electrochem.* **1987**, *225*, 49−63.
(48) Huske, M.; Stockmann, R.; Offenhausser, A.; Wolfrum, B. Redox Cycling in Nanoporous Electrochemical Devices. *Nanoscale* **2014**, *6*, 589−598.
(49) Ma, C.; Contento, N. M.; Gibson, L. R.; Bohn, P. W. Recessed Ring−Disk Nanoelectrode Arrays Integrated in Nanofluidic Structures for Selective Electrochemical Detection. *Anal. Chem.* **2013**, *85*, 9882−9888.

DOI: 10.1021/acsnano.6b00049
ACS Nano 2016, 10, 3658−3664